Journal of Magnetics 16(4), 368-373 (2011) http://dx.doi.org/10.4283/JMAG.2011.16.4.368

Determination of the Size Distribution of Magnetite Nanoparticles from Magnetic Measurements

Sunghyun Yoon*

Department of Physics, Gunsan National University, Gunsan 573-701, Korea

(Received 4 October 2011, Received in final form 25 October 2011, Accepted 26 October 2011)

Particle size distributions in 10 nm magnetite ferrofluids are analyzed based on both dc and ac magnetic measurements. Modified log-normal distributions are used for fitting the experimental results, which allows for a proper account of the narrow distributions. The calculated average particle sizes are in good agreement with the TEM results. However the ac method gives a much narrower distribution width than that of the dc magnetization curve fit. The proposed measurements combined with the analysis methods are useful for the characterization of ferrofluids being considered for biomedical applications.

Keywords : magnetic nanoparticles, magnetite, relaxation, complex magnetic susceptibility

1. Introduction

Potential applications of ferromagnetic and superparamagnetic nanoparticlces (MNPs) in biomedical research take advantage of their magnetic field response, small size and large surface-to-volume ratios. Both *in vitro* biosensor techniques and *in vivo* therapies have been proposed which make use of magnetic relaxation of the nanoparticle ferrofluids in an ac magnetic field [1]. AC magnetic biosensing techniques detect the specific binding of biomolecules to the surface of the MNPs by sensing an increase of the MNP's effective hydrodynamic volume and interactions with neighboring particles. The binding event is measured as a shift in the MNPs' relaxation frequency [2,3]. Energy losses via ac magnetic reversal or rotation of the MNP in viscous fluid can be employed for localized heating to destroy cancer cells *in vivo* (magnetic fluid hyperthermia) [4,5]. These and other applications generally require detailed knowledge and precise control of the average particle size and size distribution. Narrow size distribution is a pre-requisite for achieving the best results in the chosen application.

While transmission electron microscopy allows one to image particles directly and determine their size and distribution, it is limited by poor statistical sampling. Moreover, the particles need to be precipitated and cannot be studied in a liquid environment of direct relevance to the biological application. On the other hand extracting size and size-distribution from magnetic measurements of ferrofluids is an inexpensive and statistically significant alternative, which reflects the properties over all the part of the sample. However, the accuracy of the latter depends on the model used in the data analysis. In this study, the particle sizes and size-distributions of magnetite nanoparticle systems are determined by three complementary methods: transmission electron microscopy (TEM), dc magnetization, and ac susceptibility measurements. Improvement of the latter two methods is achieved through a realistic choice of the mathematical model for the size distribution.

*Corresponding author: Tel: +82-63-469-4562
Fax: +82-63-469-4561, e-mail: shyoon@kunsan.ac.kr

2. Background and Approach

Rotation of the magnetic moment of a particle immersed in a viscous fluid is impeded by two dissipation mechanisms of different physical origins - the fluid viscosity and the magnetic anisotropy energy barrier of the particle. The mechanism with a shorter relaxation time will dominate [6]. The measured relaxation time t is determined by the relation:

$$\frac{1}{\tau} = \frac{1}{\tau_B} + \frac{1}{\tau_N} \tag{1}$$

Here τ_B is the Brownian relaxation time of the rotation of the MNP with the *hydrodynamic* volume V_H (which

includes the adsorbed molecules on the surface) in a viscous fluid,

$$\tau_B = \frac{3\eta V_H}{k_B T}, \tag{2}$$

where η is the viscosity of the carrier fluid, k_B is the Boltzmann constant and T is the absolute temperature. The Néel relaxation time τ_N is the time needed to overcome the anisotropy energy barrier, KV_M, where K is the anisotropy constant and V_M is the *magnetic core* volume. The value of τ_N can be expressed as [7]:

$$\tau_N = \tau_0 \sigma^{-1/2} \exp(\sigma) \quad \sigma < 2 \tag{3}$$

$$t_N = \tau_0 \sigma \quad \sigma << 2 \tag{4}$$

where

$$\sigma = KV_M/k_B T, \tag{5}$$

and $\tau_0 \sim 10^{-9}$ s. For a given magnetic material and viscosity, the dominant relaxation (loss) mechanism changes from anisotropy- to viscosity-limited with increasing particle size. Figure 1 shows a variation of the effective relaxation time τ as a function of the particle size and the σ value given in Eq. (5). The calculations were done for a toluene-based magnetite ferrofluid having a uniaxial anisotropic constant of 3.7 kJ/m^3 and a viscosity of 0.5542×10^{-3} Pa·s. Particles were all assumed to be spheres and the thickness of the surfactant layer was set to 2 nm. It is apparent from the figure that, unless the particle radius exceeds 9 nm, Néel-type relaxation is dominant.

In ac experiments we measure the complex initial (that is in small fields) susceptibility $\chi = M/H = \chi' - i\chi'$ as a function of frequency. The relaxation time is determined from the *relaxation frequency* $\omega_{max} = 1/\tau$, at which the imaginary part of the magnetic susceptibility, χ'', is maximized. The frequency dependence of the complex magnetic susceptibility of an MNP array in the Debye [8] approximation is:

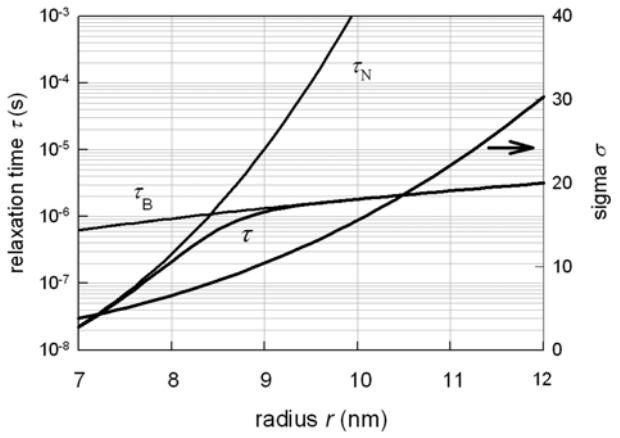

Fig. 1. Variations in the relaxation time τ (Eqs. (2), (3), and (4)) and s (Eq. (5)) with respect to the particle radius in a magnetite suspension in toluene.

$$\chi = \frac{\chi_0}{1 + i\omega\tau}, \tag{6}$$

or

$$\chi' = \frac{\chi_0}{1 + (\omega\tau)^2}, \tag{7}$$

$$\chi'' = \frac{\omega\tau}{1 + (\omega\tau)^2}\chi_0 . \tag{8}$$

The initial magnetic susceptibility at zero frequency, χ_0, is given by:

$$\chi_0 = \frac{n m_p^2}{3 k_B T}, \tag{9}$$

where n is the particle number density (and all the moments m_p are assumed equal).

In "large" field magnetization, M is a non-linear function of the field with saturation. The dependence of magnetization on the magnetic field is usually measured in dc fields. For ferrofluids composed of an ensemble of identical particles, this dependence is described by the Langevin function:

$$M(H) = \varepsilon M_S L(r, H) = \varepsilon M_S (\coth\alpha - 1/\alpha) \text{ with } \alpha = \frac{m_p H}{k_B T} \tag{10}$$

where M_S is the spontaneous magnetization of the single domain particles ($m_p = M_S V_M$) and ε is the volume fraction of MNPs in the ferrofluid

Since a real ferrofluid always has a distribution of particle sizes, these relations should be weight-averaged with a proper particle size distribution (PSD) function. Chantrell [9] presented a method that can model the *magnetization curves* of ferrofluids using a log-normal distribution function:

$$g(y) = \frac{1}{y\sigma\sqrt{2\pi}} \exp(-(\ln y)^2/2\sigma^2) \tag{11}$$

Here, σ is the standard deviation of ln y and y = d/<d> is the reduced diameter (d is the particle diameter and <d> is the mean diameter of the distribution). In Ref [9], g(y)dy is the fraction of the total magnetic volume having reduced diameters between y and y+dy. The log-normal distribution is inheretantly broad, i.e. the distribution width is typically of the order of or even larger than the mean value. Nowadays, many research groups have the ability to control the monodispersity of the ferrofluid to a much higher precision. Hence a different distribution

function is required to properly describe the sharper size distribution. We propose a modified log-normal distribution function which can be successfully used in the analyses of ferrofluids with narrow size distributions [10]:

$$g(r) = \frac{1}{(r-\theta)\sigma\sqrt{2\pi}} \exp(-\ln\{(r-\theta)/r_0\}^2/2\sigma^2). \quad (12)$$

Here a new parameter θ has been introduced to control the peak position and r_0 is the constant included for correct dimensionality. Notice that in our calculations the argument of the function g is the particle *radius* measured in nanometers, whereas y in Eq. (11) is the reduced diameter, a dimensionless quantity. This technical choice does not affect the generality of the method. The average radius <r> is defined as the first moment of the distribution, and can be calculated from θ and σ as:

$$<r> = \theta + r_0 e^{\sigma^2/2}. \quad (13)$$

We also notice that there are two alternative approaches to the description of the particle size distribution (we formulate them in terms of distribution functions defined for radii). In the first approach the distribution function $g(r)$ refers to the particle *number* fraction, that is, $g(r)$dr denotes the number of particles with radii within the range from r to r + dr. This function is useful when a size distribution histogram is obtained from a TEM image by counting the numbers of particles in different size steps, and it has been employed in analyses of magnetic data in some publications [11]. Throughout this study we are using the *volume* fraction distribution $g(r)$ following Refs. [9, 12], where $g(r)dr$ is the fraction of magnetic particles of radii in the range from dr to r + dr.

3. Experiment

Measurements were carried out on surfactant-coated MNP samples. Magnetite (Fe_3O_4) MNPs coated with oleic acid (OA) in toluene were synthesized via thermal decomposition of transition metal carbonyls in the presence of surfactant-mediated solvents at high temperature under inert atmosphere followed by mild oxidization [13-15].

DC magnetization curves were measured on a vibrating sample magnetometer (VSM) at room temperature using samples containing 60 μL of ferrofluid each. Complex ac susceptibilities were measured at room temperature in the frequency range of 40 Hz - 110 MHz by means of the slit-toroid method [16] using an HP4294A impedance analyzer. We used a high permeability toroid with a 0.35 mm slit wound with 15 turns of litz wire. The resistance and reactance of the coils were measured as a function of frequency with the gap empty, and then with the ferrofluid under investigation injected into the gap. Though the instrument allows measurements in the range 40 Hz - 110 MHz, a measurement setup resonance reduced the high frequency limit of data available for analyses by up to about 13 MHz. The oscillation level of the driving current was maintained at less than 10 mA, which was below the magnetic saturation limit of the sample ferrofluid. From these data, the real and the imaginary parts of susceptibility, χ' and χ'', were calculated following the method described in Ref. [17].

4. Results and Discussion

The TEM image in Fig. 2 shows that the nanoparticles are spherical with a narrow size distribution. The nominal average radius of the magnetite nanoparticles obtained from an analysis of the TEM micrographs was $r_{TEM} = 5$ nm.

The room temperature dc magnetization curve (Fig. 3(a)) shows non-hysteretic behavior. This is always the case in diluted ferrofluids, independent of whether the thermal fluctuations of the moment direction are dominated by particle rotation or reversal within the particle. In order to estimate the particle size and the width of the size distribution, the positive quadrant part of the curve was fitted to the classical Langevin function weight-averaged with the modified lognormal PSD of Eq. (12):

$$M(H) = \varepsilon M_S \int_0^\infty g(r) L(r, H) dr. \quad (14)$$

This equation was numerically integrated to find the values of σ and θ which give the best fit to the measured curves over the whole data range. The volumetric packing fraction ε was determined under the assumption that the

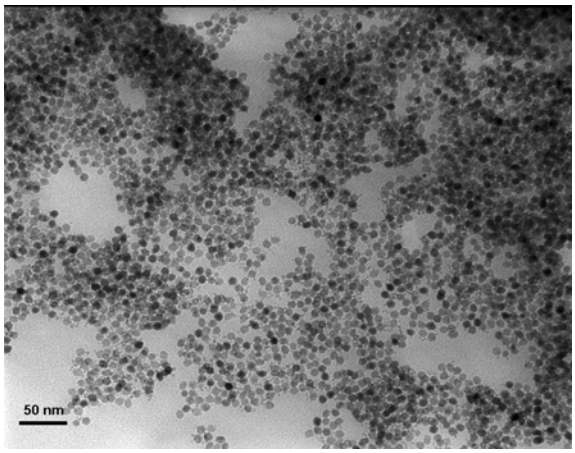

Fig. 2. TEM micrographs of 10 nm diameter magnetite nanoparticles.

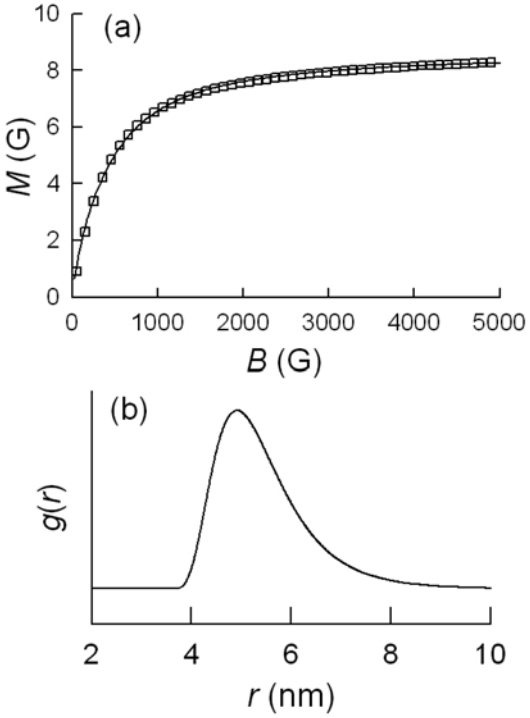

Fig. 3. Experimental results of the dc magnetization analysis for magnetite are shown in the top panel. The squares are experimental points; the solid line is obtained from calculation Eq. (14), using the particle size distribution of Eq. (12). The corresponding distribution function is shown below.

saturation magnetization of the ferrofluid MNP is the same as that of bulk material (5700 G for magnetite [18]). The experimental data and the size distribution obtained are illustrated in Fig. 3 and the results of the analysis are listed in Table 1, where the width of the distribution at the half height (HW) is also included as an intuitive parameter for easier comparison with the results of other works. The distribution profiles show a long asymmetric tail extending toward larger *r*. While larger particles are not seen in the TEM images, this tail may reflect the effect of inter-particle dipole-dipole interactions.

Fig. 4 shows the experimentally measured real and imaginary parts of the susceptibility for magnetite particles coated with OA dispersed in toluene, where f_{max} for the imaginary part is equal to 7.5 MHz. As is in accordance with the discussion concerning Fig. 1, the Néel relaxation is found to be the dominant relaxation mechanism. The

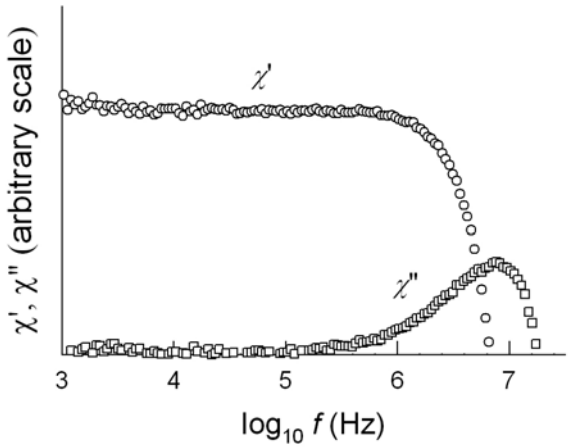

Fig. 4. Real and imaginary parts of the ac susceptibilities as a function of frequency for magnetite nanoparticles coated with OA in toluene. Circles are the real part values, χ'; squares are the imaginary part values, χ''.

Néel model gives a better fit to experimental data than the Brownian relaxation. For the latter, the relaxation frequency for these particles in toluene ($\eta = 0.5542$ mPa·s) would have been 0.76 MHz.

A close look at the shape of the measured $\chi''(\omega)$ data shows that the peak width is broader than that expected for a monodispersed array (with a single relaxation time), and shows an asymmetric tail toward low frequency, which indicates the existence of an asymmetric size distribution in the ferrofluid. The frequency dependence of the complex magnetic susceptibility of the ferrofluid is [19]:

$$\chi(\omega) = \frac{\varepsilon M_S^2}{9k_BT}\int_0^\infty \frac{g(r)r^3}{1+\omega\tau}dr\,, \tag{15}$$

from which the in-phase and the out-of-phase polydispersed susceptibilities become:

$$\chi'(\omega) = \frac{\varepsilon M_S^2}{9k_BT}\int_0^\infty \frac{g(r)r^3}{1+(\omega\tau)^2}dr\,, \tag{16}$$

$$\chi''(\omega) = \frac{\varepsilon M_S^2}{9k_BT}\int_0^\infty \frac{\omega\tau g(r)r^3}{1+(\omega\tau)^2}dr \tag{17}$$

where $g(r)$ is the same PSD function used in Eq. (12) and ε is a volumetric packing fraction of the ferrofluid. This means the frequency-dependent susceptibility of the ferro-

Table 1. Results of magnetic particle size analyses using TEM, dc magnetization and ac susceptibility measurements. The average radius obtained from the TEM image is also included for comparison.

TEM	dc magnetization				ac susceptibility				
r_{TEM} (nm)	<*r*> (nm)	σ	HW (nm)	ε(%)	<*r*> (nm)	σ	HW (nm)	$\lvert K\rvert$ (erg/cc)	f_{max} (MHz)
5.0	5.2	1.05	1.05	0.15	4.7	0.06	0.15	3.7×10^5	7.5

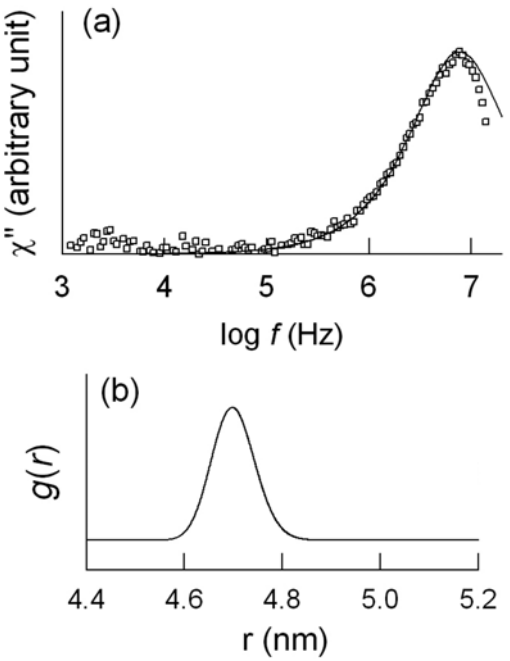

Fig. 5. Experimental results of the imaginary part of ac susceptibility analysis for magnetite nanoparticles. The squares are experimental points; the solid line is obtained from calculation Eq. (17) using particle size distribution Eq (12). The corresponding distribution is shown below.

fluid can be understood as a superposition of single-particle responses to the alternating field. Now τ is the relaxation time given by Eq. (1). Fannin [20] has assessed the theoretical contribution of the Néel relaxation by weight-averaging the susceptibilities with particle radii distributions obtained from electron microscopy. In the present study, we integrate Eq. (17) numerically using the average magnetic radius and the standard deviation values obtained from the static magnetization measurements as a starting point for the iteration procedure, to find a new set of θ and σ which give the best fit for experimental χ'' (imaginary part). We can also determine the anisotropy constant K from the analysis through Eq. (5); the calculated anisotropy constant is 3.7×10^5 erg/cm^3, which is within the range of values, 2.3~4.1 $\times 10^5$ erg/cm^3, that have been reported in the literature [11]. The experimental and simulation results are displayed in Fig. 5. The obtained particle sizes are in fair agreement both with the TEM results and fits to the analyses of the static magnetization curves. However the distributions obtained by the ac method are much narrower (see the summary of the fitting results in Table 1). This stems from the fact that the ac method is much more sensitive to the influences of the environment through motional friction or binding events. Furthermore, magnetic nanoparticles are well known to be aligned in chain-like clusters under the presence of a dc magnetic field, by which a certain degree of inter-particle magnetic dipolar interaction is reflected in the broader distribution width obtained from the dc magnetic measurement. As long as only the calculated distribution width is of concern, the ac measurement can give more accurate results with regard to the particle size. In addition, the PSD appears, to an extent, symmetric, which is anticipated because the sample has an extremely narrow distribution width.

5. Conclusion

Two methods of determining the particle size distributions for MNP ferrofluids with narrow distribution widths were described. The methods were tested with 10 nm magnetite ferrofluids. Fitting both the dc and ac data to the models with a modified log-normal distribution gives good agreement of the average particle sizes between the two methods and with the TEM results. While the ac susceptibility measurement yielded a sharper distribution than the dc magnetization measurement, it gave an average radius roughly consistent with the values obtained by using both the electron microscopy and the dc method. These methods in combination with the proposed model function for particle size distribution and the computational formalism can be applied for the characterization of magnetic nanoparticles for biomedical applications.

Acknowledgements

This work was supported by the Basic Science Research Program (2010-0023413) through the NRF of Korea.

References

[1] K. M. Krishnan, IEEE Trans. Magn. **46**, 2523 (2010).
[2] S. H. Chung, A. Hoffmann, S. D. Bader, C. Liu, B. Kay, L. Makowski, and L. Chen, Appl. Phys. Lett. **85**, 2971 (2004).
[3] Y. Bao, A. B. Pakhomov, and K. M. Krishnan, J. Appl. Phys. **99**, 08H107 (2006).
[4] Joan Connolly and Timothy G. St. Pierre, J. Magn. Magn. Mater. **225**, 156 (2001).
[5] R. Hergt, R. Hiergeist, M. Zeisberger, G. Glockl, W. Weitschies, L. P. Lamirez, I. Hilger, and W. A. Kaiser, J. Magn. Magn. Mater. **280**, 358 (2004).
[6] M. I. Shliomis, Sov. Phys.-Usp. **17**, 153 (1974).
[7] W. F. Brown, J. Appl. Phys. **34**, 1319 (1963).
[8] P. Debye, Polar Molecules, Chemical Catalog Company, New York (1929).
[9] R. W. Chantrell, J. Popplewell, and S. W. Charles, IEEE Trans. Magn. **14**, 975 (1978).

[10] S.-H. Yoon, M. Gonzales-Weimuller, Y.-C. Lee, and Kannan M. Krishnan, J. Appl. Phys. **105**, 07B507 (2009).
[11] P. C. Fannin, B. K. P. Scaife, and S. W. Charles, J. Magn. Magn. Mater. **65**, 279 (1987).
[12] R. E. Rosensweig, J. Magn. Magn. Mater. **252**, 370 (2002).
[13] M. Gonzales and K. M. Krishnan, J. Magn. Magn. Mater. **293**, 265 (2006).
[14] T. Hyeon, S. S. Lee, J.-N. Park, Y.-H. Chung, and H. B. Na, J. Am. Chem. Soc. **123**, 12798 (2001).
[15] A. G. Loca, M. P. Morales, and C. J. Serna, IEEE Trans. Magn. **42**, 3025 (2006).
[16] P. C. Fannin, B. K. P. Scaife, and S. W. Charles, J. Phys. E: Sci. Instrum. **19**, 238 (1986).
[17] P. C. Fannin, B. K. P. Scaife, and S. W. Charles, J. Magn. Magn. Mater. **72**, 95 (1988).
[18] E. P. Wohlfarth, Ferromagnetic Materials, North-Holland, Amsterdam (1982).
[19] S.-H. Yoon, J. Korean Phys. Soc. **54**, 163 (2009).
[20] P. C. Fannin and S. W. Charles, J. Phys. D: Appl. Phys. **22**, 187 (1989).